IJE TRANSACTIONS A: Basics Vol. 33, No. 4, (April 2020) 657-667

International Journal of Engineering

Journal Homepage: www.ije.ir

Design of Broaching Tool Using Finite Element Method for Achieving the Lowest Residual Tensile Stress in Machining of Ti6Al4V Alloy

P. Khanjanzadeh[a], H. Amirabadi*[a], J. Sadri[b]

[a] *Department of Mechanical Engineering, University of Birjand, Birjand, Iran*
[b] *Department of Computer Science & Software Engineering, Concordia University, Montreal, Canada*

PAPER INFO

Paper history:
Received 11 December 2019
Received in revised form 14 January 2020
Accepted 17 January 2020

Keywords:
Broaching
Finite Element Method
Machining
Ti6Al4V Alloy
Tungsten Carbide

ABSTRACT

The aim of this study, is to use finite element simulation to achieve the optimal geometry of a broaching tool that creates the lowest tensile stress at the machined surface of the Ti6Al4V alloy. It plays a major role in reducing production costs and improves the surface integrity of the machined parts. The type and amount of residual stress determined by the thermal and mechanical loads transmitted to the workpiece. In this research, the two-dimensional simulation of the broaching process is done by finite element DEFORM-2D® software for the two end teeth of the tool that perform the cutting operation. In simulating the first tooth, Response Surface Method is used to select the desired controllable parameters of the process such as cutting speed, rake angle, clearance angle, rise per tooth and depth of cut. In order to establish low thermal and high mechanical load in workpiece, multi-objective genetic algorithm employed after perform simulation in the first tooth. In simulating the second tooth, Response Surface Method used to select desired controllable parameters of the process such as rake angle, clearance angle and radius of cutting edge. For the second tooth, a multi-objective genetic algorithm has been used. Ultimately, the geometry of the broaching tool utility has been designed to store the lowest tensile residual stresses in the machined surface for Ti6Al4V alloy.

doi: *10.5829/ije.2020.33.04a.17*

1. INTRODUCTION

Broaching operations are widely used in the machining industry because both roughing and finishing operations are carried out at one step. As a result, the speed of broaching operation is greater than that of machining and milling. The main applications of broaching are to carry out operations on internal or external surfaces of parts or a combination of them. One of the interesting topics of research in simulation of broaching is to achieve the value of residual stress after the process that has a significant effect on the fatigue life of the workpiece. The two end teeth of the tool that perform the cutting operation have the greatest effect on the value of residual stres. This can be controlled by selecting appropriate cutting conditions. On the other hand, Ti6Al4V alloy is a significant engineering material for using in aerospace applications such as gas turbine engines, due to its high strength and fracture toughness in addition to its low density. It should be noted that the amount and type of residual stress in this alloy for application in turbine blade design, the importance of proper servicing of this piece during its life, high temperatures during operation, and the presence of extreme centrifugal forces, are very important. Considering the working conditions of the workpiece, the design of the broaching tool that causes the tension of the residual pressure stress or the minimum tensile stress is desirable [1].

Despite the importance of the broaching process in the manufacturing industry, relatively little research has been done on it. Here, a short background to the research carried out in the field of broaching has been presented, and studies have shown that so far, research into the design of the Ti6Al4V broaching tool, in which the

*Corresponding Author Email: *hamirabadi@birjand.ac.ir* (H. Amirabadi)

Please cite this article as: P. Khanjanzadeh, H. Amirabadi, J. Sadri, Design of Broaching Tool Using Finite Element Method for Achieving the Lowest Residual Tensile Stress in Machining of Ti6Al4V Alloy, International Journal of Engineering (IJE), IJE TRANSACTIONS A: Basics Vol. 33, No. 4, (April 2020) 657-667

tension of the work piece is considered, has not been done. Liu and Guo [2], in 2000, suggested a FEM model to estimate the effect of sequential cuts on the induced residual stress in the machined layer of stainless steel 304. Mo et al. [3], in 2005, using a Taguchi test design method and changing the broaching conditions, such as cutting angle, cutting speed, rise per tooth and coolant type, performed experimental experiments on heat resistant alloys of titanium and nickel, and the effect of each factor was studied on the main cutting force, surface fineness and wear rate of tools. Makarov et al. [4], in 2008, made an experimental comparison between tool life, tool wear and surface fineness in the EI787VD heat resistant alloy broaching operation at lower cutting speeds and cutting speeds higher than the standard (over 30 m/min). Schulze et al. [5], in 2011, in order to predict induced residual stress on the machined surface in broaching process of SAE 5120 low alloy steel, used FE simulation. Kong et al. [6], in 2011, investigated the effect of serrated chip formation on shear forces, temperature fluctuations, tool life and surface integrity during broaching of nickel base alloy GH4169. Zhang et al. [7], in 2012, using a two-dimensional finite element simulation of the Inconel 718, studied the effect of cutting parameters such as the angle of inclination and the clearance angle on shear force, and the effect of the angle of inclination and the rise for each tooth on the formation of chips inside the gullet of tool. Kishawi et al. [8], in 2012, proposed a mathematical model to estimate the required force for broaching process of AISI1045 steel based on energy analysis. Sarwar et al. [9], in 2012, experimentally investigated the effect of chip angle, clearance angles and depth of the initial cutting on the quality of the finished workpiece and the type of chip formed on titanium alloy IMI318. Jafarian et al. [10], in 2015, proposed a method for optimization of residual stress on the machined surface in turning process of Inconel718. Fabre et al. [11], in 2017, presented an innovative Lagrangian model to simulate cutting operation of AISI 1045 steel under broaching conditions, using iterative procedure. Chandrashekar and Prasad [12], in 2018, investigated the flank wear and tool life of Tungsten Carbide for turning of Ti6Al4V. Ortiz-de-Zarate et al. [13], in 2019 evaluated different flow stress laws and chip formation of Ti6Al4V under broaching conditions using finite element simulation.

Previous research has used a single tooth tool to simulate broaching tool, by which cutting operations are performed sequentially. Whereas in this study a two teeth tool is used and the cutting operations are performed by two teeth simultaneously. As a result, the effects of the first tooth on cutting operation of the second tooth are considered in every respect.

The main contribution of this manuscript is a two-fold one. 1- For the first time, the cutting operation simulation is performed simultaneously by two cutting blades. 2- Using finite element simulation to achieve the optimal geometry of a broaching tool that creates the lowest tensile stress at the machined surface of the Ti6Al4V alloy; this plays a major role in reducing production costs and improves the surface integrity of the machined parts. Based on finite element simulation, for our tool, the workpiece surface temperature (T) is and the effective strain (ES) level of the workpiece surface are 301˚C and 3.59, respectively.

2. RESEARCH METHOD

Figure 1 shows the block diagram of research method in this study.

2. 1. Design of Experiments for Simulation of cutting Operations in the First Tooth In this paper, first the cutting process in the first tooth is simulated. In order to design the experiments, response

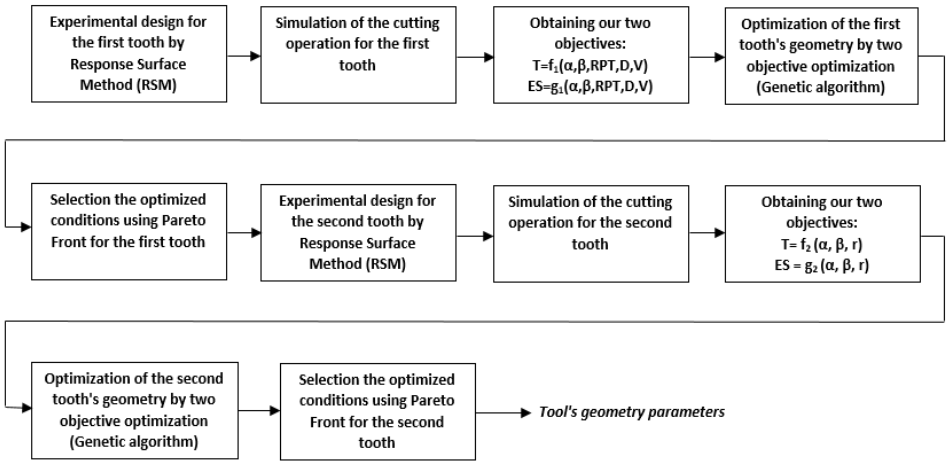

Figure 1. Block diagram of research method

surface method (RSM) is used for different cutting conditions of the first tooth. The five effective factors of our cutting mechanics are: 1- cutting speed with four levels (V = 3, 6, 9, 12 m/min); 2- clearance angles with three levels ($\alpha = 3^{\circ}, 6^{\circ}, 9^{\circ}$); 3- the rake angle with three levels ($\beta = 5^{\circ}, 15^{\circ}, 25^{\circ}$); 4- initial depth of cut, with three levels (D = 0.04, 0.07, 0.1 mm) and; 5-rise for each of the tooth with three levels (RPT = 0.02, 0.05, 0.08 mm). Columns 2-6 in Table 1, show effective factors for investigation of effect of the first tooth in simulation of cutting operations.

2. 2. Mechanical and Thermal Properties of Tool and Workpiece To achieve the mechanical and thermal properties of Ti6Al4V and cementite carbide uncoated tool, DEFORM® software database [14], is used. DEFORM-2D software has a coupled thermo-elasto-plastic Lagrangian code with continuous re-meshing. The most commonly used tools in the Ti6Al4V alloy broaching by researchers in experimental tests and simulations is made of cemented carbide because of its high useful life, lack of accumulated edge and failure to react with the workpiece [15]. Since the workpiece is

TABLE 1. Effective factors for investigation of effect of the first tooth in simulation

Test Number	Effective Factors					Outputs	
	α (degree)	β (degree)	RPT (mm)	D (mm)	V (m/min)	T (°C)	ES
1	25	6	0.05	0.07	3	230	3.77
2	15	6	0.08	0.1	9	430	4.07
3	5	3	0.02	0.04	3	262	5.17
4	5	6	0.02	0.07	3	294	6.76
5	15	9	0.02	0.07	6	334	4.87
6	5	6	0.02	0.07	12	511	4.93
7	5	3	0.05	0.07	12	466	5.10
8	15	6	0.05	0.04	9	357	4.28
9	15	9	0.02	0.07	6	334	4.87
10	25	3	0.08	0.1	12	410	3.89
11	15	3	0.02	0.1	12	483	4.62
12	5	3	0.08	0.1	3	303	6.27
13	5	9	0.08	0.1	12	505	4.62
14	5	9	0.08	0.04	3	246	4.78
15	5	9	0.02	0.1	3	320	6.20
16	25	3	0.08	0.04	3	195	4.36
17	25	9	0.08	0.04	12	329	4.78
18	25	6	0.05	0.07	3	230	3.77
19	25	9	0.08	0.1	3	237	4.46
20	15	6	0.05	0.04	9	357	4.28
21	25	9	0.02	0.04	3	210	3.50
22	5	6	0.05	0.1	6	415	5.24
23	15	3	0.08	0.07	6	316	4.36
24	15	6	0.05	0.04	9	357	4.48
25	25	3	0.02	0.1	3	252	6.39
26	5	3	0.02	0.1	9	480	5.34
27	25	3	0.02	0.04	12	341	3.32
28	15	3	0.02	0.1	12	483	4.62
29	25	9	0.02	0.1	12	416	3.88
30	5	3	0.08	0.04	12	415	5.74
31	5	9	0.02	0.04	12	443	5.08

considered as a plastic material, the yield stress curve is used to determine the behavior of the material during severe plastic deformations [16]. In order to simulate the machining process, the upgraded Lagrangian method is used first, which, by re-meshing at each step of the simulation, allows the possibility of severe plastic deformations in the workpiece. In meshing of workpiece and cutting tool, four node quadrilateral elements are used. In the simulation, cutting continues until second tooth reaches the edge of the workpiece. During this time, the temperature and machining forces have been balanced.

2. 3. Friction Modeling The frictional conditions in contact between tool and chip are normally very complicated, therefore it is important to determine its exactness in the simulation of the finite element. In Figure 2, in the cross sectional area of tool and chip, the distribution of vertical and frictional stresses are shown. Among different friction-definition models, the sticky-slippery friction model is more realistic and is more consistent with the experimental distribution of frictional stresses in the common parts of the tool. This model expresses the friction in two distinct regions which are referred to as a sticky and slippery friction zone, separately in the order shown in Equation (1). Here, τ is friction stress, μ the Coulomb friction coefficient, σ_n normal stress and k yield shear stress. In simulations in the present study, this model has been used to define friction in the contact between tools and chip, and the coefficient of friction of 0.7 in simulations has been used [16, 17].

$$\begin{cases} \tau(x) = \mu\,\sigma_n(x) & \text{when } \tau < k \\ \tau(x) = k & \text{when } \tau \geq k \end{cases} \quad (1)$$

2. 4. Validation of Simulation Results First, before performing the simulation of the broaching process to ensure that the material model and the friction conditions selected for the Ti6Al4V material and the tungsten carbide tool are correct, the accuracy of simulation results must be checked. Therefore, simulation of the two-dimensional machining process with a tooth was done by DEFORM-2D® software and the results were compared with the results of Umberllo's research in 2008 [18]. The comparison is made between the forces of machining and the shape of the chip after the operation. As shown in Figure 3, the shape of the chip obtained from Umberllo's simulation and research is acceptable.

According to Table 2, the force generated by the simulation in this study with a difference of 9.4% compared to the experimental force is comparable to that of Umberllo's simulation results. Also, in Table 3, the parameters of chip morphology such as average pitch, average peak and average valley obtained from our simulation, Umberllo's simulation and experimental results are reported.

2. 5. Response Surface Model In this study, due to the large number of parameters, the second level response model was used to find the relationship between the temperature and effective strain functions of the workpiece and dependent variables. Relationships (2) and (3), respectively, represent the temperature and effective strain functions of the workpiece.

$$\begin{aligned} T = {} & 110.56564 - 1.55014\times\alpha + 24.85248\times\beta - \\ & 1002.39300\times RPT + 400.44834\times D + 34.21281\times V \\ & - 0.000231512\times\alpha^2 - 1.84984\times\beta^2 + \\ & 7108.39556\times RPT^2 + 4258.84005\times D^2 - \\ & 0.97862\times V^2 - 0.012170\times\alpha\times\beta + \\ & 8.74462\times\alpha\times RPT - 13.15376\times\alpha\times D - \\ & 0.25326\times\alpha\times V - 4.59037\times\beta\times RPT - 26.70179\times \\ & \beta\times D - 0.061076\times\beta\times V + 120.38646\times RPT\times \\ & D - 15.45590\times RPT\times V + 6.27596\times D\times V \end{aligned} \quad (2)$$

$$\begin{aligned} ES = {} & 4.53437 - 0.10757\times\alpha - 0.056177\times\beta + \\ & 6.66978\times RPT + 49.23177\times D - 0.037643\times V \\ & - 0.000218763\times\alpha\times\beta + 0.16778\times\alpha\times RPT + \\ & 0.45766\times\alpha\times D + 0.00118946\times\alpha\times V - 0.15806\times \\ & \times RPT - 1.25545\times\beta\times D + 0.014584\times\beta\times \\ & V - 348.92503\times RPT\times D + 1.78718\times RPT\times V - \\ & 3.08611\times D\times V \end{aligned} \quad (3)$$

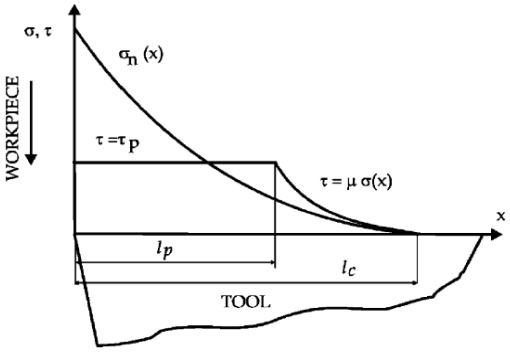

Figure 2. Stress distribution on chip surface 17

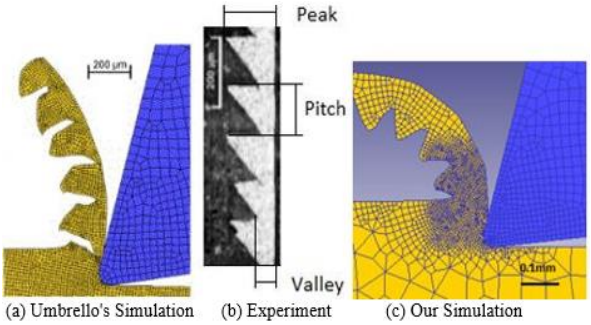

Figure 3. Comparison of chip formation in experimental and simulation results in V=120m/min, D = 0.127m/rev, (a) Umbrello's Simulation, (b) Experiment, (c) Our Simulation

TABLE 2. Comparison of forces in experimental and simulation results V=120m/min, D = 0.127 mm/rev

Our simulation force (N)	Umberllo's simulation force (N)	Experimental force (N)
506.5	602	559

TABLE 3. Comparison of chip morphology in experimental and simulation results V=120m/min, D = 0.127 mm/rev

	Average pitch (µm)	Average peak (µm)	Average valley (µm)
Experimental	140	230	46
Umberllo's simulation	149	208	43
Our simulation	144	167	59

2. 6. Optimization of Geometry of the First Tooth In this research, for the purpose of optimization, the Non-dominated Sorting Genetic Algorithm (NSGA-II), has been used. The NSGA-II is one of the most utilized and powerful algorithms available for solving multi-objective optimization problems and has been proven to be effective in solving various problems. Srinivas and Deb [19] introduced the NSGA optimization method in 1995 for solving multi-objective optimization problems.

After the first stage of simulation, in order to achieve optimal residual stress in the workpiece, two objective functions of minimum temperature and maximum mechanical load in the workpiece are selected to optimize the first tooth. Since the increase of the effective strain increases the stress, and as a result of increasing the mechanical stress transferred to the workpiece [20] the results of the simulation of the temperature and effective strain of the workpiece have been extracted. The objective functions are shown in Relations (4) and (5):

$$\textit{First objective} = \textit{workpiece temperature} \quad (4)$$

$$\textit{Second objective} = -(\textit{effective strain}) \quad (5)$$

Here, both objective functions need to be optimized. The optimally extracted Pareto front of the NSGA-II algorithm is shown in Figure 4. Each of the spots shown in Pareto front, based on effect percentage of objectives, can be optimal.

2. 7. Design of Experiments for Simulation of Cutting Operations in the Second Tooth After optimizing the first tooth, response surface method (RSM) is used to achieve different cutting conditions for the second tooth. In order to test design for the second tooth, chip angle with three levels (α = 35˚, 40˚, 45˚); clearance angle with three levels (β = 3˚, 6˚, 9˚); and the radius of the tool tip with three levels (R = 0.01, 0.02, 0.03); are used. Columns 2-4 in Table 4 show effective factors for investigation of the effect of the second tooth in simulation of cutting operation.

2. 8. Simulation of Cutting Operations for the Second Tooth In order to simulate the broaching process, the updated Lagrangian solution is used, which, by repositioning at each stage of the simulation, allows the possibility of severe plastic deformations in the workpiece. In this method, the cutting process continues until the machining forces reach stable conditions. At this stage of the study, using the Design Expert10 software, the relationships between the temperature and effective strain functions of the workpiece and dependent variables have been obtained. Equation (6) represents the temperature in terms of variables, and Equation (7) gives an effective strain in terms of variables.

$$\begin{aligned} T = &-1865.69553 + 107.86152 \times \alpha - 4.03730 \\ &\times \beta + 4805.39359 \times R - 1.33094 \times \alpha^2 - \\ &1.66613 \times \beta^2 + 72909.06379 \times R^2 + 0.36566 \\ &\times \alpha \times \beta - 220.69280 \times \alpha \times R + 515.23158 \times \\ &\beta \times R \end{aligned} \quad (6)$$

$$\begin{aligned} ES = &0.58330 + 0.43132 \times \alpha - 0.79302 \times \beta \\ &- 428.95250 \times R - 0.00849894 \times \alpha^2 - \\ &0.059147 \times \beta^2 + 5870.57933 \times R^2 + \\ &0.034099 \times \alpha \times \beta + 4.09089 \times \alpha \times R \\ &+ 12.18980 \times \beta \times R \end{aligned} \quad (7)$$

2. 9. Optimization of Geometry of the Second Tooth After the simulation of the second tooth in different cutting conditions, optimization for this tooth was performed similar to the first tooth. The objective functions are the least thermal load and the maximum mechanical load in the workpiece. The Pareto front of the optimization is shown in Figure 5. Each of the spots showed in Pareto front, based on effect percentage of objectives, can be optimal.

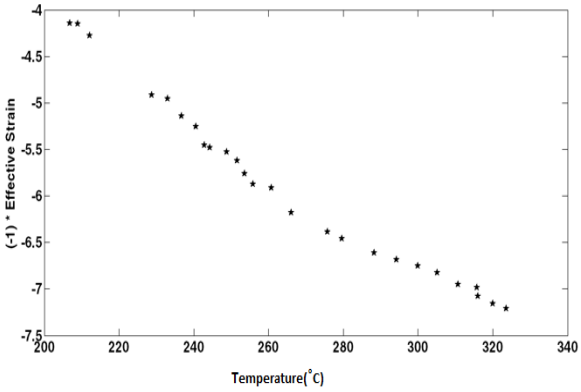

Figure 4. Pareto front resulted from multi-objective optimization by genetic algorithm for the first tooth

TABLE 4. Effective factors for investigation of effect of the second tooth in simulation

Test Numbers	Effective factors			Outputs	
	α (degree)	β (degree)	R(mm)	T (°C)	ES
1	35	3	0.03	299	3.93
2	45	6	0.03	306	5.59
3	40	9	0.01	290	3.68
4	40	6	0.03	373	4.68
5	45	3	0.03	276	3.12
6	35	3	0.01	292	3.50
7	40	6	0.03	373	4.68
8	45	9	0.03	305	6.47
9	35	6	0.02	285	3.56
10	35	9	0.03	350	4.10
11	35	6	0.02	285	3.56
12	40	3	0.01	297	3.58
13	40	3	0.02	317	3.57
14	45	9	0.02	301	3.59
15	35	3	0.02	316	3.42
16	35	6	0.01	293	4.37
17	45	6	0.01	298	4.06
18	40	9	0.01	290	3.68
19	45	6	0.01	298	4.06
20	40	3	0.02	317	3.57

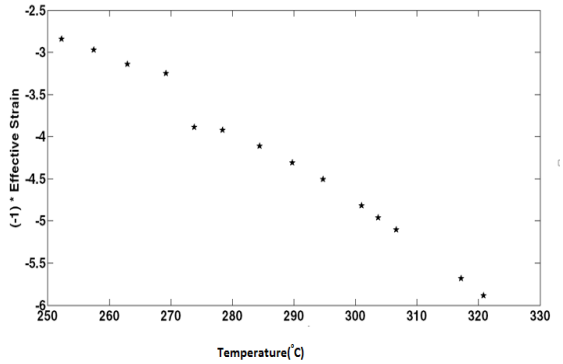

Figure 5. Pareto front resulted from multi-objective optimization by genetic algorithm for the second tooth

3. RESULTS

In this section, the simulation results, including the temperature and effective strain of the workpiece from the beginning to the mechanical stability, are presented in columns 7 and 8 of Table 1. Temperature and effective strain values at the workpiece surface are extracted for optimization after simulations.

The results of the simulations of the first tooth indicate that cutting velocity has the greatest effect on the temperature of the workpiece. After cutting speed, the workpiece temperature is affected by the depth of cut and the rise per tooth. The effective strain in the parts at the same speed, at low clearance and low chip angles, has the highest value.

The two objectives in this study are of the same importance in simulation, so the 25th row of Table 5, is selected as optimum spot. Then, simulation of the broaching process with the characteristics of the optimum spot is performed. Table 6 shows the comparison of the results from simulation and optimization.

The results of the second tooth simulation are shown in Table 4. The results from the simulation using optimal parameters for the first tooth are shown in Figure 6.

The two objectives in this study are of the same importance in simulation, so the 11th row of the Pareto-optimal front of Table 7, as optimum spot is selected. After selection, simulation of the broaching process with the characteristics is performed. Table 8 shows the comparison of the results obtained from simulation and optimization. The results obtained from the simulation

using optimal parameters for the first tooth are shown in Figure 7. Table 9 shows the comparison between the results obtained from simulation and optimization.

4. DISCUSSION

By comparing the results, it can be seen that cutting velocity is the most important factor affecting the temperature of the workpiece during broaching so that with increasing speed, the temperature in the workpiece increases significantly. Figures 8-12 show respectively the effects of cutting velocity, rake angle, clearance angle, rise per tooth and depth of cut on the workpiece temperature.

When the cutting velocity increases, the process of forming the serrated tooth chip is more evident. This process is due to the fact that the shear stress in the shear

TABLE 5. Results of optimization for the first tooth

Test Number	Effective Factors					Outputs	
	α (degree)	β (degree)	RPT (mm)	D (mm)	V (m/min)	T (°C)	ES
1	20.4	3.1	0.06	0.04	3	207	4.14
2	20.7	3.1	0.04	0.08	3	244	5.48
3	9.2	3.1	0.02	0.09	3	300	6.75
4	14.6	3.2	0.02	0.1	3	288	6.61
5	17.5	3.1	0.02	0.1	3	276	6.38
6	5.1	3.2	0.02	0.1	3	324	7.21
7	9.4	3.3	0.02	0.1	3	305	6.82
8	19.7	3.1	0.02	0.1	3	266	6.18
9	20.4	3.1	0.06	0.04	3	207	4.14
10	20.4	3.2	0.06	0.04	3	209	4.15
11	19.4	3.2	0.04	0.08	3	249	5.53
12	7.7	3.2	0.02	0.1	3	311	6.95
13	19.2	3.1	0.05	0.04	3	212	4.28
14	19.9	3.1	0.04	0.07	3	229	4.91
15	7.1	3.2	0.02	0.1	3	316	7.08
16	19.8	3.2	0.03	0.07	3	241	5.26
17	12.5	3.2	0.02	0.1	3	294	6.68
18	17.9	3.1	0.03	0.09	3	261	5.91
19	19.5	3.2	0.04	0.07	3	237	5.14
20	17.5	3.1	0.06	0.07	3	233	4.96
21	17.2	3.2	0.02	0.1	3	280	6.46
22	5.7	3.2	0.02	0.1	3	320	7.16
23	7.2	3.4	0.02	0.1	3	316	6.98
24	19.9	3.1	0.02	0.08	3	254	5.76
25	**18.4**	**3.1**	**0.04**	**0.08**	**3**	**252**	**5.62**
26	20.6	3.1	0.03	0.1	3	256	5.87
27	21.2	3.1	0.04	0.08	3	243	5.45

TABLE 6. Comparison between simulation and optimization results

	α (degree)	β (degree)	RPT (mm)	D (mm)	V (m/min)	T (°C)	ES
*	18.4	3.1	0.04	0.08	3	258	4.70
**	18.4	3.1	0.04	0.08	3	252	5.62

* Our simulation results using DEFORM10®
** Our optimal point from Pareto Front results based on NSGA-II

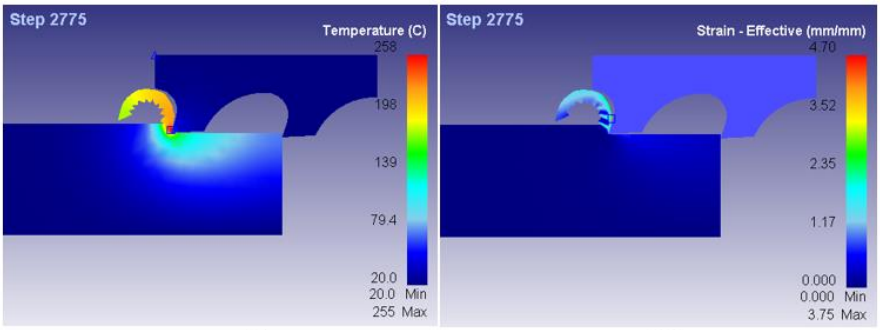

(a) (b)

Figure 6. Results of tool simulation with optimized parameters, (a) Temperature, (b) Effective strain

TABLE 7. Results of optimization for the second tooth

Test Number	α (degree)	β (degree)	R (mm)	T (˚C)	ES
1	35.0	9.0	0.01	252	2.84
2	45.0	9.0	0.03	321	5.89
3	45.0	9.0	0.03	304	4.96
4	35.1	8.4	0.01	263	3.14
5	45.0	9.0	0.01	274	3.89
6	35.4	8.2	0.01	269	3.25
7	44.9	9.0	0.02	295	4.51
8	45.0	8.9	0.02	290	4.31
9	35.2	8.8	0.01	257	2.97
10	45.0	9.0	0.03	321	5.89
11	**45.0**	**9.0**	**0.02**	**284**	**4.11**
12	35.0	9.0	0.01	252	3.84
13	45.0	9.0	0.03	317	5.68
14	45.0	9.0	0.02	301	4.82
15	44.9	9.0	0.01	278	3.93
16	45.0	9.0	0.03	307	5.11

TABLE 8. Comparison between simulation and optimization results for the second tooth

	α (degree)	β degree)	R (mm)	T (˚C)	ES
*	45	9	0.02	301	3.59
**	45	9	0.02	284	4.11

* Our simulation results using DEFORM10®
** Our optimal point from Pareto Front results based on NSGA-II

TABLE 9. The parameters of the first and second optimized teeth

Tool parameters	α (degree)	β (degree)	RPT (mm)	R (mm)	D (mm)	V (m/min)
First tooth	18.4	3.1	-	-	0.08	3
Second tooth	45.0	9.0	0.04	0.02	-	-

region increases the permeability of the workpiece (shear stress) and creates a crack area in the workpiece, where these cracks can weld together and produce serrated tooth chip. The results obtained from

simulation of cutting operation by the first tooth show that the cutting angle and clearance angle have the least effect on the temperature and effective strain of the workpiece, which is consistent with the results of Schulze's research [5]. However, among the simulation results at the same cutting speed, the workpiece which is machined by a tool with less chip angle and less clearance angle has the most effective strain.

Since the phase transformation temperature in the Ti6Al4V alloy is in the range of 800-850˚C [21], and based on simulation results, the workpiece temperature does not exceed 600 ˚C, so there is no residual stress due to phase transformation in the workpiece. The optimized geometry of the tool is shown in Figure 13. In this tool, based on finite element simulation, the workpiece surface temperature and the effective strain level of the workpiece surface are 301˚C and 3.59, respectively.

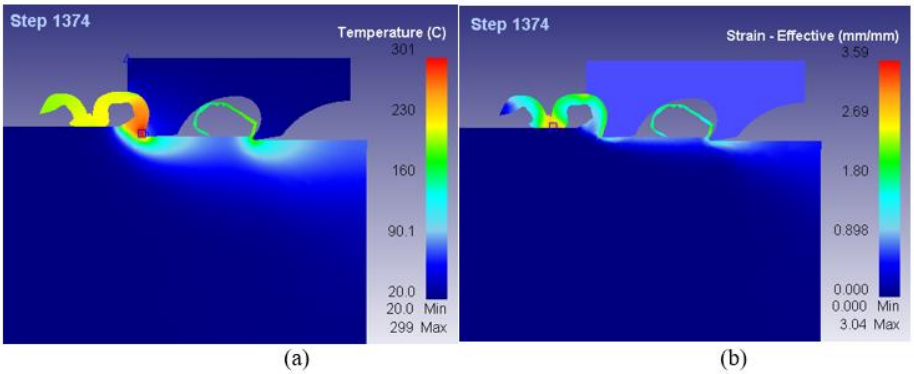

(a) (b)

Figure 7. Results of tool simulation with optimized parameters, (a) Temperature, (b) Effective strain

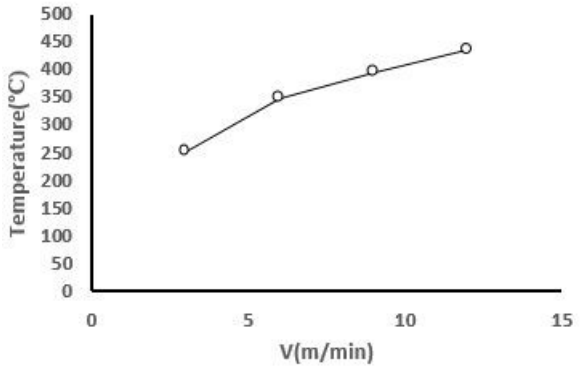

Figure 8. Effect of cutting velocity on workpiece temperature

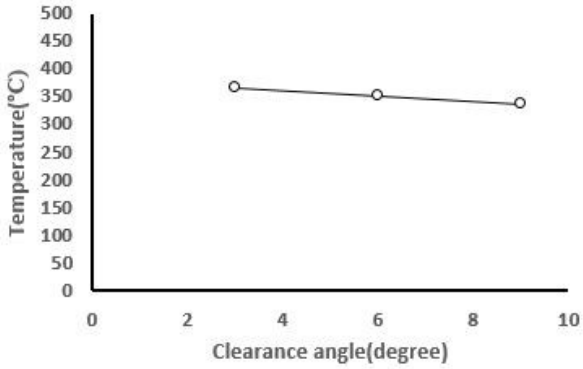

Figure 10. Effect of clearance angle on workpiece temperature

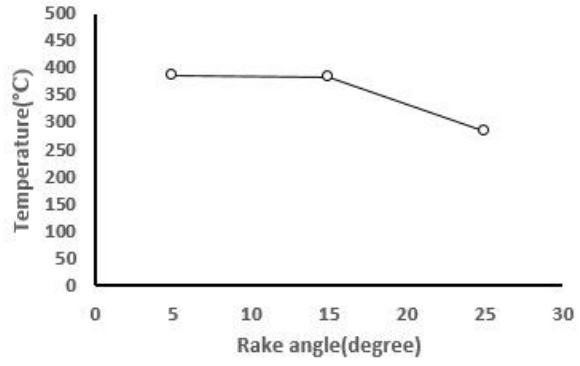

Figure 9. Effect of rake angle on workpiece temperature

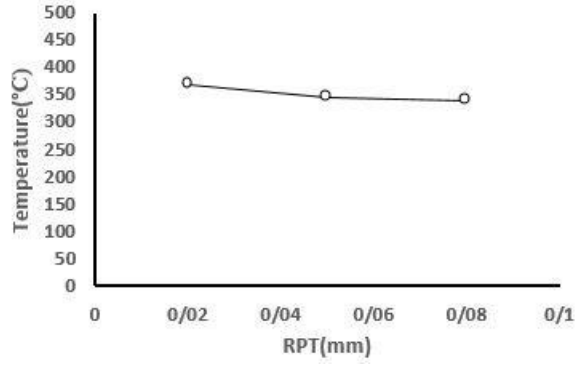

Figure 11. Effect of rise per tooth on workpiece temperature

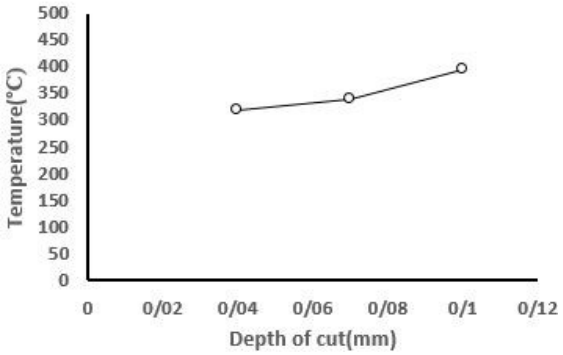

Figure 12. Effect of depth of cut on workpiece temperature

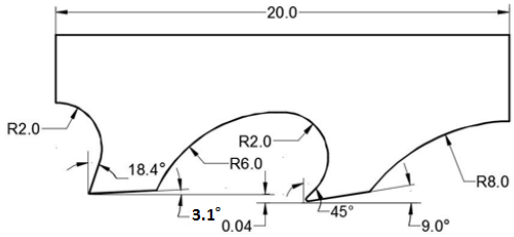

Figure 13. Designed broaching tool with optimized the last teeth

5. CONCLUSION

The aim of this study is to use finite element simulation to achieve the optimal geometry of a broaching tool that creates the lowest tensile stress in the machined surface of the Ti6Al4V alloy. The results of the simulations of the first tooth indicate that cutting velocity has the greatest effect on the temperature of the workpiece. The results from the first tooth simulation show that the cutting angle and clearance angle have the least effect on the temperature and effective strain of the workpiece, which is consistent with the results of Schulze's. Based on simulation results, at the same cutting speed, the workpiece, which is machined by a tool with less chip angle and less clearance angle, has the most effective strain. In the broaching process of Ti6Al4V, phase transformation does not occur and the effective factors in causing residual stresses in the workpiece are the mechanical and thermal loads. In the optimized tool, the workpiece surface temperature after simulation of the finite element and the effective strain level of the workpiece surface are 301˚C and 3.59, respectively.

6. REFERENCES

1. Davim, J.P., Machining: fundamentals and recent advances, Springer Science & Business Media, (2008).
2. Liu, C.R. and Guo, Y. B., "Finite element analysis of the effect of sequential cuts and tool–chip friction on residual stresses in a machined layer", ***International Journal of Mechanical Sciences***, Vol. 42, No. 6, (2000), 1069–1086.
3. Mo, S.P., Axinte, D.A., Hyde, T.H. and Gindy, N. N. Z., "An example of selection of the cutting conditions in broaching of heat-resistant alloys based on cutting forces, surface roughness and tool wear", ***Journal of materials processing technology***, Vol. 160, No. 3, (2005), 382–389.
4. Makarov, V.F., Tokarev, D.I. and Tyktamishev, V. R., "High speed broaching of hard machining materials.", ***International Journal of Material Forming***, Vol. 1, No. 1, (2008), 547–550.
5. Schulze, V., Osterried, J. and Strauß, T., "FE analysis on the influence of sequential cuts on component conditions for different machining strategies", ***Procedia Engineering***, Vol. 19, (2011), 318–323.
6. Kong, X., Li, B., Jin, Z. and Geng, W., "Broaching performance of superalloy GH4169 based on FEM", ***Journal of Materials Science & Technology***, Vol. 27, No. 12, (2011), 1178–1184.
7. Zhang, Y.L. and Chen, W.Y., "Finite Element Modeling of the Broaching Process of Inconel718", In Materials Science Forum (Vol. 697), Trans Tech Publications Ltd., (2012), 39–43.
8. Kishawy, H.A., Hosseini, A., Moetakef-Imani, B. and Astakhov, V. P., "An energy based analysis of broaching operation: Cutting forces and resultant surface integrity", ***CIRP Annals***, Vol. 61, No. 1, (2012), 107–110.
9. Sarwar, M., Dinsdale, M. and Haider, J., "Development of advanced broaching tool for machining titanium alloy", In Advanced Materials Research (Vol. 445), Trans Tech Publications Ltd., (2012), 161–166.
10. Jafarian, F., Amirabadi, H. and Sadri, J., "Experimental measurement and optimization of tensile residual stress in turning process of Inconel718 superalloy", ***Measurement***, Vol. 63, (2015), 1–10.
11. Fabre, D., Bonnet, C., Rech, J. and Mabrouki, T., "Iterative Lagrangian model of broaching to study cutting forces, temperatures and chip formation.", In AIP Conference Proceedings (Vol. 1769, No. 1), AIP Publishing LLC., (2016), 19–24.
12. Chandrashekar, M. and Prasadb, K. S., "Evaluation of Flank Wear of Iron-rich Binder Carbide Cutting Tool in Turning of Titanium Alloy", ***International Journal of Engineering-Transactions C: Aspects***, Vol. 31, No. 6, (2018), 943–948.
13. Ortiz-de-Zarate, G., Sela, A., Ducobu, F., Saez-de-Buruaga, M., Soler, D., Childs, T.H.C. and Arrazola, P. J., "Evaluation of different flow stress laws coupled with a physical based ductile failure criterion for the modelling of the chip formation process of Ti-6Al-4V under broaching conditions", ***Procedia CIRP***, Vol. 82, (2019), 65–70.
14. Theoretical Manual, DEFORM-2D-10®, (2010).
15. Ezugwu, E.O. and Wang, Z. M., "Titanium alloys and their machinability—a review", ***Journal of Materials Processing Technology***, Vol. 68, No. 3, (1997), 262–274.
16. Özel, T. and Ulutan, D., "Prediction of machining induced residual stresses in turning of titanium and nickel based alloys with experiments and finite element simulations", ***CIRP Annals***, Vol. 61, No. 1, (2012), 547–550.
17. Filice, L., Micari, F., Rizzuti, S. and Umbrello, D., "A critical analysis on the friction modelling in orthogonal machining", ***International Journal of Machine Tools and Manufacture***, Vol. 47, No. 3–4, (2007), 709–714.
18. Umbrello, D., "Finite element simulation of conventional and high speed machining of Ti6Al4V alloy", ***Journal of Materials Processing Technology***, Vol. 196, No. 1–3, (2008), 79–87.
19. Srinivas, N. and Deb, K., "Muiltiobjective optimization using nondominated sorting in genetic algorithms", ***Evolutionary Computation***, Vol. 2, No. 3, (1994), 221–248.

20. Deb, K., Pratap, A., Agarwal, S. and Meyarivan, T. A. M. T., "A fast and elitist multiobjective genetic algorithm: NSGA-II", ***IEEE Transactions on Evolutionary Computation***, Vol. 6, No. 2, (2002), 182–197.

21. Smith, W.F., Structure and properties of engineering alloys, McGraw-Hill, (1993).

Persian Abstract

چکیده

هدف از این مطالعه، استفاده از شبیه‌سازی اجزائ محدود برای دست‌یابی به هندسه‌ی بهینه یک ابزار خان‌کشی است که کمترین تنش کششی را در سطح ماشین‌کاری شده آلیاژ Ti6Al4V ایجاد کند. این امر نقش مهمی در کاهش هزینه های تولید و بهبود یکپارچگی سطح قطعات ماشین‌کاری شده دارد. نوع و میزان تنش باقی‌مانده با استفاده از بارهای حرارتی و مکانیکی ایجاد شده در قطعه کار تعیین می‌شود. در این پژوهش شبیه‌سازی دوبعدی فرایند خان‌کشی، با استفاده از نرم‌افزار المان محدود DEFORM-2D® برای دو دندانه‌ی انتهایی ابزار صورت گرفته است. در شبیه‌سازی عملیات برشی دندانه‌ی اول برای تعیین میزان تاثیر هر یک از پارامترهای قابل کنترل در فرایند از جمله سرعت برش، زاویه‌ی براده، زاویه‌ی آزاد، افزایش ارتفاع در هر دندانه و عمق برش از روش سطح پاسخ (RSM) استفاده شده است. به منظور ایجاد بار حرارتی کم و بار مکانیکی بالا در قطعه کار، الگوریتم ژنتیک چندهدفه به کار گرفته شده است. در شبیه‌سازی عملیات برشی دندانه‌ی دوم برای تعیین میزان تاثیر هر یک از پارامترهای قابل کنترل در فرایند از جمله زاویه‌ی براده، زاویه‌ی آزاد و شعاع لبه‌ی برش از روش سطح پاسخ استفاده شده است. برای دندانه‌ی دوم نیز به منظور بهینه‌سازی بارهای حرارتی و مکانیکی ایجاد شده در قطعه کار، الگوریتم ژنتیک چندهدفه به کار گرفته شده است. در نهایت، هندسه‌ی ابزار خان‌کشی برای ایجاد کمترین تنش باقی‌مانده‌ی کششی در سطح ماشین‌کاری شده برای آلیاژ Ti6Al4V طراحی گردیده است.